HHS Public Access

Author manuscript

Nanomedicine. Author manuscript; available in PMC 2019 June 01.

Published in final edited form as:

Nanomedicine. 2018 June ; 14(4): 1381–1394. doi:10.1016/j.nano.2018.04.008.

Hyaluronic acid conjugated nanoparticle delivery of siRNA against TWIST reduces tumor burden and enhances sensitivity to cisplatin in ovarian cancer

Sophia A. Shahin, PhD[a,b], **Ruining Wang, PhD**[d,1], **Shirleen I. Simargi, MS**[b,c,1], **Altagracia Contreras, BS**[b,e], **Liliana Parra, MS**[b], **Louise Qu, DVM**[a,b], **Wei Wen, PhD**[f], **Thanh Dellinger, MD**[f], **Juli Unternaehrer, PhD**[g], **Fuyuhiko Tamanoi, PhD**[h], **Jeffrey I. Zink, PhD**[d], and **Carlotta A. Glackin, PhD**[a,b]

[a]Irell & Manella Graduate School of Biological Sciences, City of Hope – Beckman Research Institute, 1500 E. Duarte Road, Duarte, California 91010, USA, Tel: (+1)626-256-4673

[b]Department of Stem Cell and Developmental Biology, City of Hope – Beckman Research Institute, 1500 E. Duarte Road, Duarte, California 91010, USA, Tel: (+1)626-256-4673

[c]Department of Biological Sciences, California State University, Pomona, CA 91768, Tel: (+1)-909- 869-4038

[d]Department of Chemistry and Biochemistry, California NanoSystems Institute, University of California Los Angeles, 405 Hilgard Avenue, Los Angeles, California 90095–1569, USA, Tel: (+1)-310–825-1001; Fax: (+1)-310–206-4038

[e]Department of Biological Sciences, California State University, Long Beach, CA 90840, Tel: (+1)-562-324-8800

[f]Department of Surgery, City of Hope – Beckman Research Institute, 1500 E. Duarte Road, Duarte, California 91010, USA, Tel: (+1)626-256-4673

[g]Department of Biochemistry, Loma Linda University School of Medicine, Loma Linda, CA 92350, Tel: (+1)-909-558-7691; Fax:(+1)-909-558-4887

[h]Department of Microbiology, Immunology, and Molecular Genetics, Jonsson Comprehensive Cancer Center, California NanoSystems Institute, University of California Los Angeles, 405 Hilgard Avenue, Los Angeles, California 90095–1569, USA, Tel: (+1)-310–206-7318; Fax: (+1)-310–206-5231

Abstract

TWIST protein is critical to development and is activated in many cancers. TWIST regulates epithelial-mesenchymal transition, and is linked to angiogenesis, metastasis, cancer stem cell

Correspondence to: Carlotta A. Glackin.

[1]Co-second authors; these authors contributed equally to this work.

phenotype, and drug resistance. The majority of epithelial ovarian cancer (EOC) patients with metastatic disease respond well to first-line chemotherapy but most relapse with disease that is both metastatic and drug resistant, leading to a five-year survival rate under 20%. We are investigating the role of TWIST in mediating these relapses. We demonstrate TWIST-siRNA (siTWIST) and a novel nanoparticle delivery platform to reverse chemoresistance in an EOC model. Hyaluronic-acid conjugated mesoporous silica nanoparticles (MSN-HAs) carried siTWIST into target cells and led to sustained TWIST knockdown *in vitro*. Mice treated with siTWIST-MSN-HA and cisplatin exhibited specific tumor targeting and reduction of tumor burden. This platform has potential application for overcoming clinical challenges of tumor cell targeting, metastasis and chemoresistance in ovarian and other TWIST overexpressing cancers.

Graphical Abstract

siRNA targeting TWIST can be complexed by electrostatic interactions with polyethyleneimine (PEI) coated mesopourous silica nanoparticle (MSN) conjugated with hyaluronic-acid (HA). Delivery of the MSN-HA-siTWIST into Ovcar8 cells resulted in substantial TWIST knockdown and sensitization of cells to chemotherapy treatment. *In vivo* studies demonstrated that MSN-HAs carrying TWIST siRNA demonstrated effective cancer stem cell targeting via its native ligand, CD44; and MSN-HA-siTWIST combined with cisplatin produced greater reduction in tumor growth and burden than cisplatin or MSN-siTWIST alone.

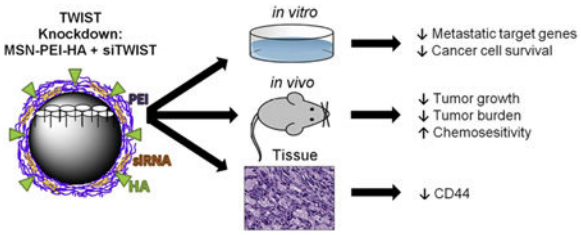

Keywords

TWIST; siRNA; mesoporous silica nanoparticle; hyaluronic acid; ovarian cancer

Background

Recurrent epithelial ovarian cancer (EOC) is almost uniformly lethal. EOC is responsible for 90% of all cancers of the ovaries[1]; and about 70% of women diagnosed with EOC are already considered to be in advanced stage[1]. Despite successful initial surgery and chemotherapy, over 65% of advanced EOC will reoccur, and only 15-30% of recurrent disease will respond to chemotherapy [2-5]. To this end, tumor recurrence and metastases are primarily responsible for treatment failure in over 90% of patients with metastatic disease[6]. Thus, recurrent metastatic disease is a major clinical challenge without effective therapy. The cancer stem cell (CSC) hypothesis explains the difficulty of treating these cancers. Rare cells within a tumor exhibit characteristics of stem cells [7]. These CSC sustain mutations that allow for expression of embryonic factors that contribute to chemoresistance and metastasis [8, 9]. Currently, no EOC therapies target the CSC specifically. Until such therapies are developed, recurrent tumors will remain untreatable.

Chemoresistant CSC have been shown to be the leading cause of relapse and metastasis in many cancers[10]. Activation of several mechanisms in CSCs, including drug efflux or inactivation, signaling pathways that enhance survival, and altered DNA damage response, is known to lead to chemoresistance[9]. Moreover, EOC tumors express high levels of epithelial-mesenchymal transition (EMT) markers such as *TWIST*, which play a vital role in cancer metastasis (Figure 1A) [11, 12]. *TWIST* is found to upregulated in almost all metastatic cancers, including ovarian [12-14]. Furthermore, is it well known that TWIST and EMT control chemoresistance and stemness in cancer [15-17] (Figure 1B). TWIST expression directly affects EMT markers by overexpressing N-cadherin and vimentin, and down-regulating E-cadherin (Figure1B) [18]. Our group has shown knockdown of *TWIST* leads to reduced tumor growth, burden, and angiogenesis in melanoma [19], and abridged the invasive phenotype in triple-negative breast cancer [20]. However, nuclear localization makes targeting transcription factors such as TWIST nearly impossible with small molecule drugs[21]. To bypass this problem, we emply small interfering RNAs (siRNAs). We have developed a therapeutic siRNA against *TWIST* (Figure 1C), and have designed a novel nanoparticle-based delivery platform to specifically target CSCs. We created a polyethylenimine (PEI) coated mesoporous silica nanoparticle (MSN) conjugated with hyaluronic acid (MSN-HA). We have previously shown effective delivery to tumor cells using a similar modality, both *in vitro* and *in vivo* of ovarian, melanoma, and breast cancer [19, 20, 22].

In this study, we aimed to build upon our previous work utilizing MSN nanoparticle therapy and introduce our novel siTWIST conjugated MSN-HA technology to a highly metastatic ovarian cancer model. We hypothesized MSN-HA-siTWIST would knock down *TWIST* and sensitize CSC to chemotherapeutics via HA-CSC targeting of its native ligand, CD44. Additionally, we studied the tumor-specific targeting capability of our MSN-HAs resulting in significant selectivity, with better delivery efficiency and improved antitumor therapeutic effect as compared to current delivery systems, such as viral and non-viral vectors or lipid and polymer vesicles[10, 22-25]. We certify this novel MSN-HA-siTWIST drug delivery platform a promising therapy to inhibit metastasis and acquired drug resistance in cancer.

Methods

Cell Culture

F2 and Ovcar8 cell lines were grown in RPMI 1640 (10% fetal bovine serum and 1% penicillin/streptomycin) (Genesee Scientific) in a tissue culture incubator at 37°C, 5% CO_2, and 90% humidity. Cells were passaged every 2-4 days using 0.25% trypsin (Genesee Scientific). Where indicated, cells were transfected with Lipofectamine 2000 (Thermo Fisher). F2 cells are cisplatin resistant cells taken from primary patient tissue with high grade serous ovarian cancer and were a gift from Dr. Gil Mor at Yale University.

Optimization of Ovcar8 for in vivo use

For mouse experiments, Ovcar8 cells were stably transfected with CMV-p:EGFP-ffluc pHIV7 as described previously [26]. This resulted in expression of an eGFP-firefly luciferase (ffluc) fusion protein. Furthermore, to increase engraftment efficiency and homogeneity of the cell population, Ovcar8 cells were passaged through mice. Ovcar8-GFP+ffluc cells were

injected intraperitoneally (IP) and allowed to form tumors. Cells were harvested after 37 days and used to establish the Ovcar8-IP line.

siRNA design

siRNAs against TWIST were designed based on shRNAs that were previously validated [18, 20]. Sequences are: si419 guide, 5′-AAUCUUGCUCAGCUUGUCCUU-3′ and si419 passenger, 5′-GGACAAGCUGAGCAAGAUU-3′. Non-targeting control siRNA (siQ) was AllStars Negative Control siRNA, labeled with AlexaFluor-647 from Qiagen. For *in vivo* studies, 2′-O-methyluracil and inverted abasic ribose chemical modifications were made to the si419 passenger strand, as illustrated in Figure 3A [19].

MSN-HA design and delivery

MSNs were synthesized utilizing the sol-gel method as described previously [19, 23]. First, 250mg 95% cetyltrimethylammonium bromide (CTAB) was dissolved in 120ml of water with 875μl 2M sodium hydroxide solution, at 80°C. Next, 1.2ml of 98% tetraethylorthosilicate was added. After 15 min, 300μl of 42% 3-(trihydroxysilyl) propyl methylphosphonate was added, and the resulting mixture was stirred for 2hrs. Particles were collected using centrifugation and washed with methanol. Acidic methanol was then used to remove any remaining CTAB surfactants. Zeta potential at 50μg/mL was 43.75mV [19] (Aldrich, St. Louis, MO). Particles were ~120 nm in diameter, with 2.5nm pores. 1.8 kD-polyethyleneimine (PEI) was electrostatically attached to the particle surface to provide positive charge, to which negatively charged siRNA is attached. HA is covalently bonded to the amine groups in the PEI using EDC-NHS coupling reaction [27]. To complex siRNA for *in vitro* experiments, 10μl siRNA at 10μM was mixed with 70ul MSNs at 500μg/ml and 20μl water. The mixture was incubated overnight at 4°C on a roller. The following day, 100μl of MSN-siRNA was added to each well of a 6-well plate containing 1900μl normal medium.

Fluorescent MSNs were prepared by adding 500μl DyLight 680 NHS-Ester that reacted with the MSN amine groups. After dye labeling, the particles were thoroughly washed and dispersed in ethanol for later surface coating.

Fluorescence Microscopy

To verify cell uptake of the nanoparticle-siRNA complexes, cells were imaged immediately before harvesting. Phase and fluorescent images to detect siQ-AlexaFluor-647 were done using a Nikon TE-2000S-microscope and SPOT Advanced software (Diagnostic Instruments).

Confocal Microscopy

Ovcar8-IP cells were seeded into a 3.5 cm glass bottom tissue culture dish. Following attachment (24hr), 2ml of fresh medium replaced the old medium. Next, MSN-HA-siQ (labeled with AlexaFluor® 647) was added to the cells at final concentration of 17.5ng/μl (MSN) and 5 nM (siQ) and incubated for an additional 48. Cells were then treated with LysoTracker Red (Thermo Fisher Scientific). Confocal images were obtained using the Zeiss LSM700 Confocal Microscope (Zeiss AG).

Western Blotting

Following Lipofectamine 2000 or MSN-HA delivery of siRNA, cells were pelleted and lysed in RIPA buffer. Protein concentration was determined by BCA assay (Thermo Fisher). Following SDS-PAGE, protein was transferred to Amersham PVDF membrane (Genesee Scientific) using a BioRad Trans-Blot SD semi-dry transfer unit. Blots were then blocked in milk for one hour at room temperature or overnight at 4°C. Incubation with primary antibody took place for one hour at room temperature or overnight at 4°C, Antibodies were diluted in 5% milk, with 0.1-0.2% Tween-20. Antibodies used were TWIST 2c1a (Santa Cruz Biotechnology, Dallas, TX) at 1:250-1:500 dilution, β-Actin, A1978 (Sigma Aldrich) at 1:2500-1:5000 dilution; and Horseradish Peroxidase (HRP) conjugated anti-mouse secondary antibodies. For westerns, the Syngene Pxi4 digital blot imager and Michigan Diagnostics FemtoGlow chemilumescent substrate were used.

Sulphorhodamine B Cell Survival Assays

Ovcar8-IP cells were plated in 6 well plates and allowed to adhere overnight. The following day, cells were transfected with siQ or MSN-HA-si419. After 48-72 hours, cells were transferred to 96 well plates at 5,000 cells per well and allowed to adhere overnight. The following day cells were treated with cisplatin at a series of concentrations (cells not treated with cisplatin served as controls). After 72 hours, cells were fixed in 10% trichloroacetic acid for 1 hour at 4°C, washed with water, and dried. Cells were stained in 0.4% sulphorhodamine B (SRB) in 1% acetic acid for 15 minutes at room temperature and then washed 3-4 times with 1% acetic acid until no further color was present in the wash. Any stray SRB on the walls of the wells was removed, and stained cells were dried for 10 minutes. SRB was solubilized in 10 mM Tris base and color intensity was quantified by absorbance at 570 nm. Each condition was normalized to its own untreated control.

Animal Studies

The animal studies conducted in these experiments were done in accordance with the protocol approved by the Institutional Animal Care and Use Committee at the City of Hope Beckman Research Institute. High quality humane care for all animal subjects was implemented for this study. A total of 60 female NOD.Cg-*Prkdc*^{scid}*Il2rg*^{tm1Wjl}/SzJ (NSG) mice (The Jackson Laboratory, Bar Harbor, ME) were used. Ten-week-old mice were administered an IP of 2.5×10^6 Ovcar8-IP cells in 200 μl of RPMI media. For all studies, mice were placed into five groups: MSN-HA-siQ, MSN-HA-siTWIST, CISPLATIN, MSN-siTWIST + cisplatin, and MSN-HA-siTWIST + cisplatin (n=8 or n=12). Previous reports show no cellular uptake without MSNs [19], thus a siRNA-only group was not added to this study.

Bioluminescent imaging of mice (using Xenogen IVIS 100 biophotonic imaging system, STTARR) commenced seven days after injection of tumor cells in order to ensure engraftment, and continued once a week for four weeks. Mice were given a 100 μl IP injection of 20 mg/ml D-Luciferin (PerkinElmer, Waltham, MA). Ten minutes after the D-luciferin injection, mice were anesthetized with isoflurane (2%-5%) and placed in the biophotonic imager, and images were taken within two minutes. An alfalfa-free version of

the regular rodent diet (alfalfa-free CA-1) was administered to the siQ mice to prevent autofluorescence from the regular diet.

Intravenous (IV) versus intraperitoneal (IP) injections of MSN-HA-siRNA were conducted one week after the inoculation of Ovcar8-IP cells and done once or twice per week for a total of seven weeks. Mice received 105μl of 500ng/μl MSN complexed with 15μl of 10μM siRNA per week, with one full dose (n=8 and n=12, respectively). This is equivalent to 2.5mg MSN/week. Weekly 3mg/kg IP cisplatin injections were given starting two weeks after initial inoculation of tumor cells to ensure all mice received same amount of chemotherapy.

Lastly, animals were euthanized via CO_2 asphyxiation followed by necropsy. Both primary tumors and disseminated masses were dissected from adjacent tissue and weighed. Mice were imaged for biodistribution studies. Tumors, spleen, kidney, uterus and liver were imaged *ex vivo* to detect the location of both the Ovcar8-IP cells and MSN-HA. Efficacy data is presented from mice dosed once per week with MSN-HA-siRNA.

Pathology

Hematoxylin and eosin (H&E) and CD44 staining was conducted on tumor samples obtained at necropsy and were processed in The Pathology Core Laboratory at the City of Hope Department of Pathology and Laboratory Medicine.

Quantitative PCR

Total cellular RNA was isolated using the RNeasy Plus kit (Qiagen). An equal amount of RNA for all conditions was used as a template for cDNA synthesis using the iScript cDNA Synthesis kit with provided random primers (Bio-Rad, Hercules, CA). Quantitative RT-PCR (qPCR) was performed in triplicate using 500 ng/well cDNA and Maxima SYBR Green Master Mix (Thermo Fisher Scientific) in 25 μL reactions. Cycling was conducted in a Bio-Rad iQ5 thermal cycler for 40 cycles (95°C, 15 s; 57°C, 60 s; 79°C, 30 s) followed by melt curve analysis. Data were analyzed using Bio-Rad iQ5 software ($2^{-\Delta\Delta Ct}$ method, normalized to β-Actin).

Statistics

All *in vivo* data was analyzed using one-way ANOVA with correction for multiple comparisons, comparing all groups to CISPLATIN treatment group. Additionally, an unpaired t-test with Welch's correction was used to compare tumor number and weight between cisplatin alone and the combination cisplatin + si419H treatment groups. All analyses were done using Prism 6 software: * $p < .05$, ** $p < .01$, *** $p < .001$, **** $p < .0001$

Results

MSN-HA delivered siRNA knocks down TWIST in vitro in an ovarian cancer model

Our previous work demonstrated the efficacy of our siRNA targeting TWIST (si419 sequence in Figure 1C) [19, 20, 22]. Thus, we utilized Lipofectamine 2000 transfection to

examine the effect of si419 in Ovcar8-IP-eGFP cells. TWIST expression was knockdown over 90% within 24 hours and completely inhibited as soon as 72 hours (Figure 1D). Once our si419 was validated, we built upon our recent success with MSNs and introduced MSN-HAs as a delivery vehicle, due to the fact that without a carrier, no siRNA enters target cells (Figure 1E). The MSN-HA specifically targets CSCs through its native ligand CD44 [25, 28, 29]. Much work has focused on attempting to target CD44 in an attempt to improve drug delivery to only malignant tissue and reduce off-target affects. The PEI is electrostatically attached to the MSN surface to provide positive charge, to which negatively charged siRNA is subsequently attached. Hyaluronic acid is covalently bond to the amine groups in the PEI using EDC-NHS coupling reaction and seen using TEM [27] (Figure 2A, B and Supplementary Figure 1). In order to verify that MSN-HAs successfully delivered siRNA into target cells, we conjugated MSN-HAs with AlexaFluor-647 tagged siQ control siRNA. Microscopy revealed increased cell uptake of labeled siRNA in Ovcar8-IP-eGFP cells (Figure 2C). Our previous studies show 0.000082 mgs of the original 0.0001mgs siRNA delivered remain on the MSN in culture [23]. Furthermore, MSN-HA complexed with siTWIST (MSN-HA-siTWIST) successfully knocked down TWIST within 24 hours post transfection, and successfully uptake into cells as soon as an hour (Figure 2D, Supplementary Figure 2).

Optimization of siTWIST sequence for in vivo therapy evaluation

In order to improve siRNA uptake *in vivo*, it was reformed to bypass the issues of nuclease degradation and immune activation by siRNAs. We achieved this by chemically modifying the si419 passenger strand to create si419 hybrid siRNA (si419H, Figure 3A). In order to promote nuclease resistance of the siRNA duplex, 2′-O-methyl and inverted abasic ribose (iaB) modifications were added [30, 31]. iaB avoids the loading of the passenger strand into RISC, which then improves the potency of siRNA by safeguarding which duplexes bind to TWIST mRNA, leading to efficient knockdown and successful silencing of TWIST[30].

MSN-HAs efficiently deliver siRNA and knockdown TWIST leading to chemosensitivity of ovarian cancer cells

Confocal microscopy demonstrated that treatment of MSN-HA to Ovcar8-IP-eGFP cells resulted in siQ co-localizing in the late endosomes and lysosomes of the cells, as evidenced by LysoTracker dye overlay (Figure 3B). Specifically, this is the perinuclear space of the cell, which was expected and have previously revealed [19, 20, 22]. Transfection of MSN-HA-siTWIST in both Ovcar8-IP-eGFP and F2 cells caused robust knockdown of TWIST as soon as 24 hours (Figure 3D). Furthermore, sulphorhodamine B (SRB) based cell survival assays revealed sensitization of both ovarian cancer cell lines to standard chemotherapy, cisplatin, following MSN-HA-mediated TWIST (MSN-HA-siTWIST) knockdown (Figure 3C, data only shown for Ovcar8-IP-eGFP cells). Cisplatin resistant cells were significantly sensitized to the drug, with approximately one log difference in IC_{50} (~60 to ~5 μM).

Ovarian tumor growth is significantly inhibited by MSN-HA-siTWIST and chemo combination therapy

Mice were treated weekly for seven weeks with MSN-HA-siQ, MSN-HA-siTWIST, CISPLATIN alone, MSN-siTWIST + cisplatin, or MSN-HA-siTWIST + cisplatin. After

seven weeks of therapy, mice in the negative control (siQ) group established significant tumors which metastasized as illustrated by bioluminescent photon flux measurements (Figure 4). The mice in the siTWIST treatment group produced relatively smaller tumors, with a 40% drop in bioluminescent signal after seven weeks of therapy in comparison to the siQ controls. The chemotherapy only treatment mouse group (CISPLATIN only) was left with 60% less tumor than the siQ control. MSN-siTWIST with cisplatin, without HA, provided similar results to our previous studies[32], reducing tumor volume an additional 20% compared to cisplatin alone; whereas the MSN-HA-siTWIST with cisplatin chemotherapy treatment group (MSN-HA-siTWIST + cisplatin) exhibited the most promising outcome, with almost 90% decrease in tumor burden as compared to the siQ control and measured by bioluminescence (Figure 4).

The intraperitoneal cavity of mice from the MSN-HA-siTWIST + cisplatin group was substantially healthier when compared to MSN-HA-siQ control mice (Figure 6A). Moreover, MSN-HA-siQ control mice developed great amounts of tumor, metastasis, and ascites as compared to MSN-HA-siTWIST + cisplatin group (Figure 5 A-C) which showed no large dispersed lesions. It is important to note that cisplatin + MSN-siTWIST hindered cancer growth by almost 50%, cumulatively, (Figure 5, A-C), as shown previously[32]. However, MSN-HA-siTWIST + cisplatin combination therapy inhibited tumor growth to an even more significant degree, with almost a 75% drop in number of tumor in comparison to CISPLATIN alone and 90% compared to controls (Figure 5, A-C). A similar trend was seen for proportion of mice developing ascites and metastasis (Figure 5 B-C). Administration of the therapy, IP vs. IV did not appear to affect the positive outcome of reduced tumor burden (Figure 5D).

MSN-HA-siTWIST combination therapy demonstrated EMT inhibition in ovarian tumors

Collected tumors were analyzed for the relative mRNA quantities of TWIST, Vimentin, N-Cadherin, and E-Cadherin (EMT markers). There was a significant reduction in the amount of TWIST, Vimentin, and N-Cadherin in the MSN-HA-siTWIST cisplatin combination therapy treated mice when compared to the control mice (MSN-HA-siQ) (Figure 6, B-D). The average relative reduction of TWIST and N-Cadherin for MSN-HA-siTWIST + cisplatin mice was less than that of those treated with MSN-siTWIST + cisplatin (no HA) ($P = 0.001$), though no significant difference was observed for Vimentin or E-Cadherin. Thus, these data suggest inhibition of EMT is promising through the delivery of TWIST siRNA utilizing MSN-HA as a delivery vehicle.

MSN-HAs only accumulate at tumor sites with no evidence of off targeting effects

In order to determine if our novel MSN-HAs specifically localized at CSC tumor sites *in vivo*, we performed fluorescent imaging of siQ treated mice at necropsy. Ovcar8-IP-eGFP cells successfully produced primary tumors (ovaries) and at metastatic sites (Figure 7 B, D and F). Moreover, MSN-HAs carrying siRNA only penetrated and accumulated inside these primary tumors and metastatic sites (Figure 7 C and F), and not in any other peritoneal tissue (Figure 8) or organ examined. Most importantly, tumor uptake of MSN-HAs was significantly greater than that of MSNs without HA (Figure 7 B and C) in the primary tumor site (ovary). This data validates the increased targeting effect HA provides to the tumor sites.

Moreover, overlay of GFP (tumor) and DYLIGHT (MSN-HA) fluorescent filters further confirms MSN-HAs only accumulate at tumor sites with no evidence off targeting signal (Figure 7F, 8A-C). Lastly, CD44 antibody staining confirms MSN-HA to CD44 CSC specific targeting (Figure 8D).

Discussion

Our data elucidate a mechanism of CSC regulation in EOC via MSN-HA-siTWIST chemo-combination therapy, and proposes treatment strategies that specifically target CSCs to arrest recurrent metastatic disease. We have developed a treatment strategy that specifically targets CSCs to halt recurrent metastatic disease. Currently, no EOC therapies target CSCs specifically. These cancer-related events include cancer invasion, metastasis, and resistance to apoptotic signals, including chemotherapy. The process of EMT allows epithelial cancer cells to undergo a phenotypic switch that confers upon these otherwise polarized and immobile cells the capacity to become migratory and highly invasive mesenchymal cells [33]. Thus in cancer, EMT is a pre-requisite for metastasis [34]. In addition to the metastatic process, research in EMT has focused in two additional areas: 1) the correlation between stemness and EMT; [35-38] 2) the association between EMT and the development of drug resistance [39-42]. This work provides increasing evidence suggesting a relationship between EMT, stemness, and drug resistance and there is a need to understand how these processes correlate and how chemotherapy may accelerate these changes. The outcome of this work may provide important insight into these biological processes.

Among numerous drug delivery systems, such as viral and non-viral vector, or lipid and polymer vesicles, nanoparticles are a preferred method of choice due to their vast applications in medicine. MSNs are proven effective delivery vehicles of DNA vectors and siRNA therapeutics. Viral and non-viral vectors have been investigated for gene silencing[10]; however, numerous studies have shown that viral vectors are associated with concerns of systemic toxicity and immunogenicity, even when locally injected into the tumor site[10, 43]. Non-viral vectors are considered safer, however MSNs have large surface area, tunable pore sizes, and encapsulate molecules such as drugs[10, 25, 28, 29, 43]. Lastly, silica has high electron contrast compared to polymers which facilitate TEM analysis and enables quantification of the loading efficiency of siRNA[10, 24, 25, 43].

To our knowledge, this is the first example of silencing TWIST utilizing a novel MSN-HA delivery system in ovarian cancer models. Here we show the efficacy of chemically-modified-siRNA for *in vivo* use against TWIST in EOC models. Moreover, we demonstrate substantial TWIST knockdown utilizing MSN-HA-siTWIST *in vitro*. TWIST has been shown to be significantly associated with metastasis, EMT, drug resistance, and poor prognosis [12, 44-47], thus making it an optimal target for ovarian cancer therapy. We and others have shown that the effective knockdown of TWIST leads to a decrease in motility, followed by an increase in chemotherapy sensitivity in ovarian cancer [22, 32, 47]. The delivery of our siRNA by MSN-HA was shown to have a profound effect on both TWIST silencing and chemoresistance in the EOC model (Figure 3 C-D). These data add to the growing evidence that TWIST is a clinically significant therapeutic target for the treatment of EOC and other solid tumors.

MSN-siTWIST alone demonstrated sufficient delivery of siRNA cargo into ovarian cancer cells *in vitro* and led to substantial knockdown of TWIST and chemosensitivity *in viv*o (Figures 4 and 5) as compared to previous studies[22]. However, the substantial improvement of ovarian tumor chemosensitivity, reduction in tumor burden and profound CSC tumor localization made by the MSN-HA-siTWIST *in vivo* cannot be ignored (Figure 5 and 7). Thus, this work validates si419H's increased efficacy both *in vitro* and *in vivo* via the utilization of MSN-HA-siTWIST. Moreover, fluorescence microscopy demonstrated proper localization of MSN-HAs in the lysosomes of Ovcar8-IP-eGFP cells (Figure 3B), and provided efficacious silencing of TWIST within 24 hours and complete absence of expression within one week (Figure 3D), leading to significant chemosensitivity (Figure 3C) *in vitro*. These findings strongly support our assertion that TWIST is an important therapeutic target in ovarian cancer.

The great benefit of our system is safety and high specificity. The MSN-HA + siRNA only localize to tumor sites and not to other tissues or organs, and do so at a significantly greater rate than MSNs without HA. We have demonstrated that that PEI coating on the nanoparticle facilitates MSN uptake into tumor cells [48]. We suggest the possibility that tumor associated macrophages are moderately responsible for the MSN-HA tumor targeting and efficacy we have seen here and previously, however further research is needed to determine this stance. By conducting treatments both IV and IP, we were able to conclude no significant difference in effective therapy outcome (Figure 5D); thus, supporting the IP route of administration in current human trials and its model for effective TWIST targeting. TWIST is an embryonic protien and is silenced in adult tissues, limiting on-target, off-tumor effects of the siRNA strategy, making IP injection of MSN-HA-siTWIST an advantageous therapy. Furthermore, this work supports previous research that MSNs are safe and non-toxic at the concentrations utilized in this experiment[19, 49, 50]. Examination of most intraperitoneal organs at necropsy (uterus, heart, lung, spleen, liver, or kidney) revealed no harm to the specimens, as supported and reviewed by a certified veterinary pathologist. However, more work needs to be done on the possible side effects caused by the siRNA, if any.

The future for these MSN-HAs is bright due to their significantly improved tumor targeting and uptake compared to MSN alone, and their mesoporous nature as likened to other metal based nanoparticles, such as gold or carbon. Additional work will exploit the MSN pore structure by examining the potential to create nanovalves on the MSNs themselves that could potentially encompass an open/close function so anticancer drugs can be stored in the pores. Other work has shown the possibility for chemo drugs to be released when MSNs encounter a low pH or an external provocation such as an oscillating magnetic field [51-56].

Overall, this project serves to demonstrate that MSN-HAs can also be modified with targeting moieties such as hyaluronic acid (HA). Since HA is a native ligand for CD44, which is overexpressed and correlates with worse prognosis in EOC [57, 58], we showed here enhanced uptake into tumors, especially in primary tumors, which in previous work showed limited siRNA uptake *in vivo*[22]. Thus, an MSN-HA-siRNA approach can deliver a substantial advantage in an EOC model, and paves the way for future developments of IP therapy delivery for ovarian cancer. Future work will continue to build upon our previous

work in order to study multifunctional MSNs, combining chemo drug delivery, in various cancer models.

Supplementary Material

Refer to Web version on PubMed Central for supplementary material.

Acknowledgments

The authors thank Laura Ratliff and Tamara Tran, Animal Tumor Model Core, Light Microscopy, and Digital Imaging Core at City of Hope. Moreover, the Veterinary Pathology Core performed pathological analysis on mouse specimens.

Funding: This work was funded by a City of Hope Excellence Award and Grant EDUC2-08383 from California Institute for Regenerative Medicine (Glackin); and the National Institute of Health (Zink/Tamanoi). The Pathology Core is supported by the NCI of the NIH under award number P30CA033572. The content is solely the responsibility of the authors and does not necessarily represent the official views of the NIH.

References

1. Siegel RL, Miller KD, Jemal A. 2016; Cancer statistics, 2016. CA: a cancer journal for clinicians. 66:7–30. [PubMed: 26742998]
2. Markman M, Markman J, Webster K, Zanotti K, Kulp B, Peterson G, Belinson J. 2004; Duration of response to second-line, platinum-based chemotherapy for ovarian cancer: implications for patient management and clinical trial design. J Clin Oncol. 22:3120–3125. [PubMed: 15284263]
3. Chang SJ, Hodeib M, Chang J, Bristow RE. 2013; Survival impact of complete cytoreduction to no gross residual disease for advanced-stage ovarian cancer: a meta-analysis. Gynecol Oncol. 130:493–498. [PubMed: 23747291]
4. Coleman RL, Monk BJ, Sood AK, Herzog TJ. 2013; Latest research and treatment of advanced-stage epithelial ovarian cancer. Nature reviews Clinical oncology. 10:211–224.
5. Aghajanian C, Goff B, Nycum LR, Wang YV, Husain A, Blank SV. 2015; Final overall survival and safety analysis of OCEANS, a phase 3 trial of chemotherapy with or without bevacizumab in patients with platinum-sensitive recurrent ovarian cancer. Gynecol Oncol. 139:10–16. [PubMed: 26271155]
6. Ushijima K. 2010; Treatment for recurrent ovarian cancer-at first relapse. J Oncol. 2010:497429. [PubMed: 20066162]
7. Beck B, Blanpain C. 2013; Unravelling cancer stem cell potential, *Nat. Rev.* Cancer. 13:727–738. [PubMed: 24060864]
8. Daley GQ. 2008; Common themes of dedifferentiation in somatic cell reprogramming and cancer. Cold Spring Harb Symp Quant Biol. 73:171–174. [PubMed: 19150965]
9. Abdullah LN, Chow EK. 2013; Mechanisms of chemoresistance in cancer stem cells. Clin Transl Med. 2:3. [PubMed: 23369605]
10. Cornelison R, Llaneza DC, Landen CN. 2017; Emerging Therapeutics to Overcome Chemoresistance in Epithelial Ovarian Cancer: A Mini-Review. International journal of molecular sciences. 18
11. Terauchi M, Kajiyama H, Yamashita M, Kato M, Tsukamoto H, Umezu T, Hosono S, Yamamoto E, Shibata K, Ino K, Nawa A, Nagasaka T, Kikkawa F. 2007; Possible involvement of TWIST in enhanced peritoneal metastasis of epithelial ovarian carcinoma. Clin Exp Metastasis. 24:329–339. [PubMed: 17487558]
12. Yang J, Mani SA, Donaher JL, Ramaswamy S, Itzykson RA, Come C, Savagner P, Gitelman I, Richardson A, Weinberg RA. 2004; Twist, a master regulator of morphogenesis, plays an essential role in tumor metastasis. Cell. 117:927–939. [PubMed: 15210113]
13. Yin G, Alvero AB, Craveiro V, Holmberg JC, Fu HH, Montagna MK, Yang Y, Chefetz-Menaker I, Nuti S, Rossi M, Silasi DA, Rutherford T, Mor G. 2013; Constitutive proteasomal degradation of

TWIST-1 in epithelial-ovarian cancer stem cells impacts differentiation and metastatic potential. Oncogene. 32:39–49. [PubMed: 22349827]

14. Gort EH, Suijkerbuijk KP, Roothaan SM, Raman V, Vooijs M, van der Wall E, van Diest PJ. 2008; Methylation of the TWIST1 promoter, TWIST1 mRNA levels, and immunohistochemical expression of TWIST1 in breast cancer. Cancer epidemiology, biomarkers & prevention : a publication of the American Association for Cancer Research, cosponsored by the American Society of Preventive Oncology. 17:3325–3330.
15. Vesuna F, Lisok A, Kimble B, Raman V. 2009; Twist modulates breast cancer stem cells by transcriptional regulation of CD24 expression. Neoplasia (New York, NY). 11:1318–1328.
16. Yin G, Chen R, Alvero AB, Fu HH, Holmberg J, Glackin C, Rutherford T, Mor G. 2010; TWISTing stemness, inflammation and proliferation of epithelial ovarian cancer cells through MIR199A2/214. Oncogene. 29:3545–3553. [PubMed: 20400975]
17. Ahmed N, Abubaker K, Findlay J, Quinn M. 2010; Epithelial mesenchymal transition and cancer stem cell-like phenotypes facilitate chemoresistance in recurrent ovarian cancer. Current cancer drug targets. 10:268–278. [PubMed: 20370691]
18. Li S, Kendall SE, Raices R, Finlay J, Covarrubias M, Liu Z, Lowe G, Lin YH, Teh YH, Leigh V, Dhillon S, Flanagan S, Aboody KS, Glackin CA. 2012; TWIST1 associates with NF-kappaB subunit RELA via carboxyl-terminal WR domain to promote cell autonomous invasion through IL8 production. BMC Biol. 10:73. [PubMed: 22891766]
19. Finlay J, Roberts CM, Dong J, Zink JI, Tamanoi F, Glackin CA. 2015; Mesoporous silica nanoparticle delivery of chemically modified siRNA against TWIST1 leads to reduced tumor burden. Nanomedicine : nanotechnology, biology, and medicine. 11:1657–1666.
20. Finlay J, Roberts CM, Lowe G, Loeza J, Rossi JJ, Glackin CA. 2015; RNA-based TWIST1 inhibition via dendrimer complex to reduce breast cancer cell metastasis. BioMed research international. 2015:382745. [PubMed: 25759817]
21. Bobbin ML, Rossi JJ. 2016; RNA Interference (RNAi)-Based Therapeutics: Delivering on the Promise? Annual review of pharmacology and toxicology. 56:103–122.
22. Roberts CM, Shahin SA, Wen W, Finlay JB, Dong J, Wang R, Dellinger TH, Zink JI, Tamanoi F, Glackin CA. 2017; Nanoparticle delivery of siRNA against TWIST to reduce drug resistance and tumor growth in ovarian cancer models. Nanomedicine : nanotechnology, biology, and medicine. 13:965–976.
23. Hom C, Lu J, Liong M, Luo H, Li Z, Zink JI, Tamanoi F. 2010; Mesoporous silica nanoparticles facilitate delivery of siRNA to shutdown signaling pathways in mammalian cells. Small (Weinheim an der Bergstrasse, Germany). 6:1185–1190.
24. Hoppenot C, Eckert MA, Tienda SM, Lengyel E. 2017Who are the long-term survivors of high grade serous ovarian cancer? Gynecologic oncology.
25. Li B, Li Q, Mo J, Dai H. 2017; Drug-Loaded Polymeric Nanoparticles for Cancer Stem Cell Targeting. Frontiers in Pharmacology. 8:51. [PubMed: 28261093]
26. Brown CE, Starr R, Martinez C, Aguilar B, D'Apuzzo M, Todorov I, Shih CC, Badie B, Hudecek M, Riddell SR, Jensen MC. 2009; Recognition and killing of brain tumor stem-like initiating cells by CD8+ cytolytic T cells. Cancer Res. 69:8886–8893. [PubMed: 19903840]
27. Meng H, Xue M, Xia T, Ji Z, Tarn DY, Zink JI, Nel AE. 2011; Use of size and a copolymer design feature to improve the biodistribution and the enhanced permeability and retention effect of doxorubicin-loaded mesoporous silica nanoparticles in a murine xenograft tumor model. ACS nano. 5:4131–4144. [PubMed: 21524062]
28. Qin W, Huang G, Chen Z, Zhang Y. 2017; Nanomaterials in Targeting Cancer Stem Cells for Cancer Therapy. Frontiers in Pharmacology. 8:1. [PubMed: 28149278]
29. Mattheolabakis G, Milane L, Singh A, Amiji MM. 2015; Hyaluronic acid targeting of CD44 for cancer therapy: from receptor biology to nanomedicine. Journal of drug targeting. 23:605–618. [PubMed: 26453158]
30. Behlke MA. 2008; Chemical modification of siRNAs for in vivo use. Oligonucleotides. 18:305–319. [PubMed: 19025401]

31. Czauderna F, Fechtner M, Dames S, Aygun H, Klippel A, Pronk GJ, Giese K, Kaufmann J. 2003; Structural variations and stabilising modifications of synthetic siRNAs in mammalian cells. Nucleic Acids Res. 31:2705–2716. [PubMed: 12771196]
32. Roberts CM, Shahin SA, Loeza J, Dellinger TH, Williams JC, Glackin CA. 2017; Disruption of TWIST1-RELA binding by mutation and competitive inhibition to validate the TWIST1 WR domain as a therapeutic target. BMC cancer. 17:184. [PubMed: 28283022]
33. Mani SA, Guo W, Liao MJ, Eaton EN, Ayyanan A, Zhou AY, Brooks M, Reinhard F, Zhang CC, Shipitsin M, Campbell LL, Polyak K, Brisken C, Yang J, Weinberg RA. 2008; The epithelial-mesenchymal transition generates cells with properties of stem cells. Cell. 133:704–715. [PubMed: 18485877]
34. Thiery JP, Sleeman JP. 2006; Complex networks orchestrate epithelial-mesenchymal transitions. Nat Rev Mol Cell Biol. 7:131–142. [PubMed: 16493418]
35. Lu H, Clauser KR, Tam WL, Frose J, Ye X, Eaton EN, Reinhardt F, Donnenberg VS, Bhargava R, Carr SA, Weinberg RA. 2014; A breast cancer stem cell niche supported by juxtacrine signalling from monocytes and macrophages. Nat Cell Biol. 16:1105–1117. [PubMed: 25266422]
36. Ye X, Tam WL, Shibue T, Kaygusuz Y, Reinhardt F, Ng Eaton E, Weinberg RA. 2015; Distinct EMT programs control normal mammary stem cells and tumour-initiating cells. Nature. 525:256–260. [PubMed: 26331542]
37. Ye X, Weinberg RA. 2015; Epithelial-Mesenchymal Plasticity: A Central Regulator of Cancer Progression. Trends in cell biology. 25:675–686. [PubMed: 26437589]
38. Fabregat I, Malfettone A, Soukupova J. 2016; New Insights into the Crossroads between EMT and Stemness in the Context of Cancer. Journal of clinical medicine. 5
39. Wang X, Ling MT, Guan XY, Tsao SW, Cheung HW, Lee DT, Wong YC. 2004; Identification of a novel function of TWIST, a bHLH protein, in the development of acquired taxol resistance in human cancer cells. Oncogene. 23:474–482. [PubMed: 14724576]
40. Brozovic A. 2016The relationship between platinum drug resistance and epithelial-mesenchymal transition. Archives of toxicology.
41. Brozovic A, Duran GE, Wang YC, Francisco EB, Sikic BI. 2015; The miR-200 family differentially regulates sensitivity to paclitaxel and carboplatin in human ovarian carcinoma OVCAR-3 and MES-OV cells. Molecular oncology. 9:1678–1693. [PubMed: 26025631]
42. Stojanovic N, Brozovic A, Majhen D, Bosnar MH, Fritz G, Osmak M, Ambriovic-Ristov A. 2016; Integrin alphavbeta3 expression in tongue squamous carcinoma cells Cal27 confers anticancer drug resistance through loss of pSrc(Y418). Biochim Biophys Acta. 1863:1969–1978. [PubMed: 27108184]
43. Marchetti C, Ledermann JA, Benedetti Panici P. 2015; An overview of early investigational therapies for chemoresistant ovarian cancer. Expert opinion on investigational drugs. 24:1163–1183. [PubMed: 26206420]
44. Helleman J, Smid M, Jansen MP, van der Burg ME, Berns EM. 2010; Pathway analysis of gene lists associated with platinum-based chemotherapy resistance in ovarian cancer: the big picture. Gynecol Oncol. 117:170–176. [PubMed: 20132968]
45. Yoshida J, Horiuchi A, Kikuchi N, Hayashi A, Osada R, Ohira S, Shiozawa T, Konishi I. 2009; Changes in the expression of E-cadherin repressors, Snail, Slug, SIP1, and Twist, in the development and progression of ovarian carcinoma: the important role of Snail in ovarian tumorigenesis and progression. Medical molecular morphology. 42:82–91. [PubMed: 19536615]
46. Zhu DJ, Chen XW, Zhang WJ, Wang JZ, Ouyang MZ, Zhong Q, Liu CC. 2015; Twist1 is a potential prognostic marker for colorectal cancer and associated with chemoresistance. American journal of cancer research. 5:2000–2011. [PubMed: 26269759]
47. Zhu X, Shen H, Yin X, Long L, Xie C, Liu Y, Hui L, Lin X, Fang Y, Cao Y, Xu Y, Li M, Xu W, Li Y. 2016; miR-186 regulation of Twist1 and ovarian cancer sensitivity to cisplatin. Oncogene. 35:323–332. [PubMed: 25867064]
48. Xia T, Kovochich M, Liong M, Meng H, Kabehie S, George S, Zink JI, Nel AE. 2009; Polyethyleneimine coating enhances the cellular uptake of mesoporous silica nanoparticles and allows safe delivery of siRNA and DNA constructs. ACS nano. 3:3273–3286. [PubMed: 19739605]

49. Ferris DP, Lu J, Gothard C, Yanes R, Thomas CR, Olsen JC, Stoddart JF, Tamanoi F, Zink JI. 2011; Synthesis of biomolecule-modified mesoporous silica nanoparticles for targeted hydrophobic drug delivery to cancer cells. Small (Weinheim an der Bergstrasse, Germany). 7:1816–1826.

50. Lu J, Liong M, Zink JI, Tamanoi F. 2007; Mesoporous silica nanoparticles as a delivery system for hydrophobic anticancer drugs. Small (Weinheim an der Bergstrasse, Germany). 3:1341–1346.

51. Ambrogio MW, Thomas CR, Zhao YL, Zink JI, Stoddart JF. 2011; Mechanized silica nanoparticles: a new frontier in theranostic nanomedicine. Accounts of chemical research. 44:903–913. [PubMed: 21675720]

52. Deng ZJ, Morton SW, Ben-Akiva E, Dreaden EC, Shopsowitz KE, Hammond PT. 2013; Layer-by-layer nanoparticles for systemic codelivery of an anticancer drug and siRNA for potential triple-negative breast cancer treatment. ACS nano. 7:9571–9584. [PubMed: 24144228]

53. Dong J, Xue M, Zink JI. 2013; Functioning of nanovalves on polymer coated mesoporous silica Nanoparticles. Nanoscale. 5:10300–10306. [PubMed: 24056925]

54. Lu J, Li Z, Zink JI, Tamanoi F. 2012; In vivo tumor suppression efficacy of mesoporous silica nanoparticles-based drug-delivery system: enhanced efficacy by folate modification. Nanomedicine : nanotechnology, biology, and medicine. 8:212–220.

55. Tarn D, Xue M, Zink JI. 2013; pH-responsive dual cargo delivery from mesoporous silica nanoparticles with a metal-latched nanogate. Inorganic chemistry. 52:2044–2049. [PubMed: 23391170]

56. Thomas CR, Ferris DP, Lee JH, Choi E, Cho MH, Kim ES, Stoddart JF, Shin JS, Cheon J, Zink JI. 2010; Noninvasive remote-controlled release of drug molecules in vitro using magnetic actuation of mechanized nanoparticles. Journal of the American Chemical Society. 132:10623–10625. [PubMed: 20681678]

57. Elzarkaa AA, Sabaa BE, Abdelkhalik D, Mansour H, Melis M, Shaalan W, Farouk M, Malik E, Soliman AA. 2016; Clinical relevance of CD44 surface expression in advanced stage serous epithelial ovarian cancer: a prospective study. Journal of cancer research and clinical oncology. 142:949–958. [PubMed: 26762850]

58. Kayastha S, Freedman AN, Piver MS, Mukkamalla J, Romero-Guittierez M, Werness BA. 1999; Expression of the hyaluronan receptor, CD44S, in epithelial ovarian cancer is an independent predictor of survival. Clin Cancer Res. 5:1073–1076. [PubMed: 10353740]

Abbreviations

EOC	Epithelial ovarian cancer
EMT	Epithelial to mesenchymal transition
CSC	Cancer Stem Cell
PEI	Polyethyleneimine
MSN	Mesoporous silica nanoparticle
HA	Hyaluronic-acid
siQ	Control siRNA
CTAB	cetyltrimethylammonium bromide
siRNA	Small interfering RNA
SRB	Sulphorhodamine B
NSG	NOD.Cg-*Prkdc*^{scid}*Il2rg*^{tm1Wjl}/SzJ

IP	Intraperitoneal
IV	Intravenous
GFP	Green Fluorescent Protein
Ffluc	Firefly Luciferase
RISC	RNA Induced Silencing Complex

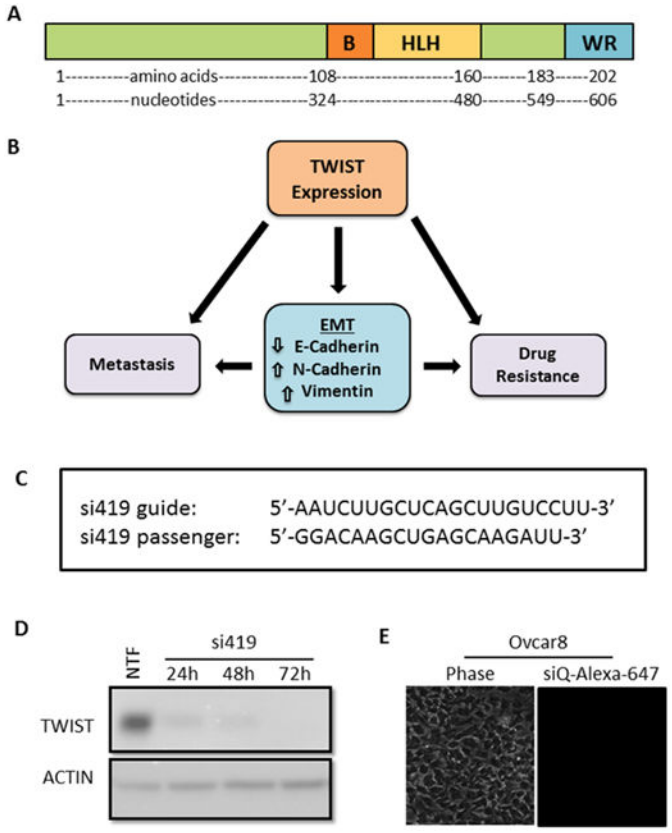

Figure 1.

A. TWIST schematic showing the basic DNA binding domain, helix-loop-helix dimerization motif, and C-terminal protein-binding WR domain. **B.** Reactivation of TWIST in cancers induces an epithelial to mesenchymal transition (EMT), which has been shown to lead to metastasis and acquired drug resistance. **C.** Sequences of TWIST siRNA (si419) targeting the coding region of TWIST mRNA. **D.** Validation of siRNA. Lipofectamine 2000 was used to transfect Ovcar8 cells with si419. Western blot reveals robust TWIST knockdown over three days post transfection. Non-transfection (NTF) is shown as a positive control for knockdown. **E.** Without a carrier, no siRNA enters target cells.

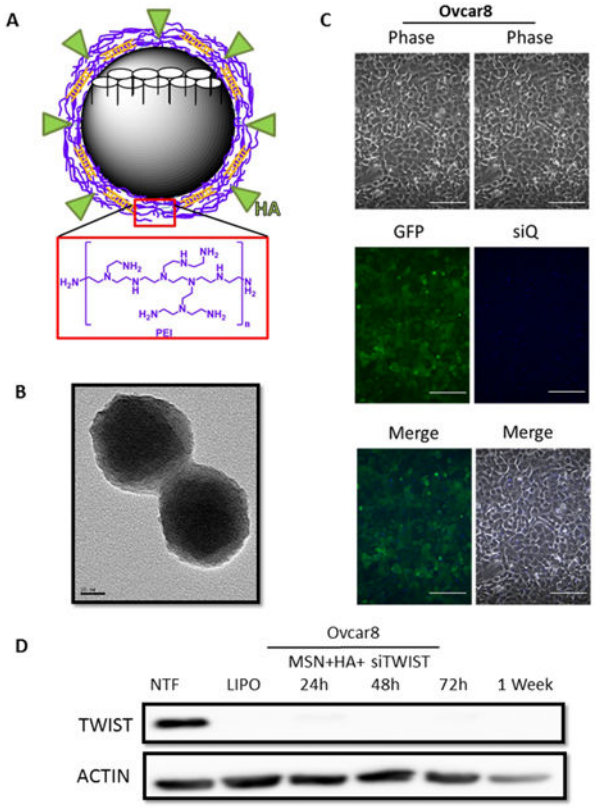

Figure 2.

A. Schematic of an MSN-HA with pore structure (white). MSN-HAs used in these studies have a PEI coating (purple layer) which allow for a balance of charge interactions to chemically bind siRNA (orange) and hyaluronic acid (HA) (green). Monomer structure for PEI is shown below (red box). **B.** Transmission electron micrograph of MSN-HAs. Particles are of uniform diameter, ~120 nm. **C.** Ovcar8-IP eGFP ffluc cells efficiently take up MSN-HAs loaded with siQ-AlexaFluor-647. Scale bar, 100 μm. **D.** si419 loaded onto MSN-HAs produce highly efficient TWIST knockdown as early as 24 hours and lasting one week post transfection. NTF and Lipofectamine were used as negative and positive controls, respectively.

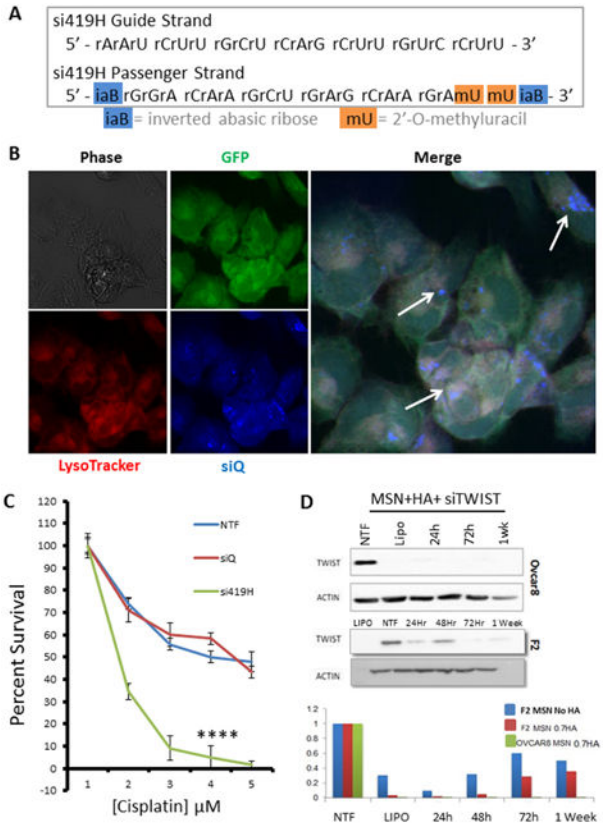

Figure 3.

A. In preparation for *in vivo* studies, si419 was chemically modified to include 2′-O-methyluracil and inverted abasic ribose caps on the passenger strand. This siRNA is termed si419H. **B.** Confocal microscopy demonstrates MSN-HA delivery of si419H into Ovcar8-IP cells. siQ-AlexaFluor-647 (blue) colocalizes with lysosomes and late endosomes, as stained by LysoTracker (red), reflecting proper endosomal trafficking of MSN-HAs to allow siRNA release. **C.** SRB cell survival assay reveals that TWIST knockdown via MSN-HAs significantly sensitizes Ovcar8-IP cells to cisplatin (P=.00018). **D.** Western blot confirms that si419H knocks down TWIST in Ovcar8-IP cells and F2 cells. Knockdown is still effective one week post treatment. Comparison of MSNs alone vs MSN-HAs reveals greater knockdown efficacy when using MSN-HAs (0.7 gr HA per 10 mg MSN-PEI).

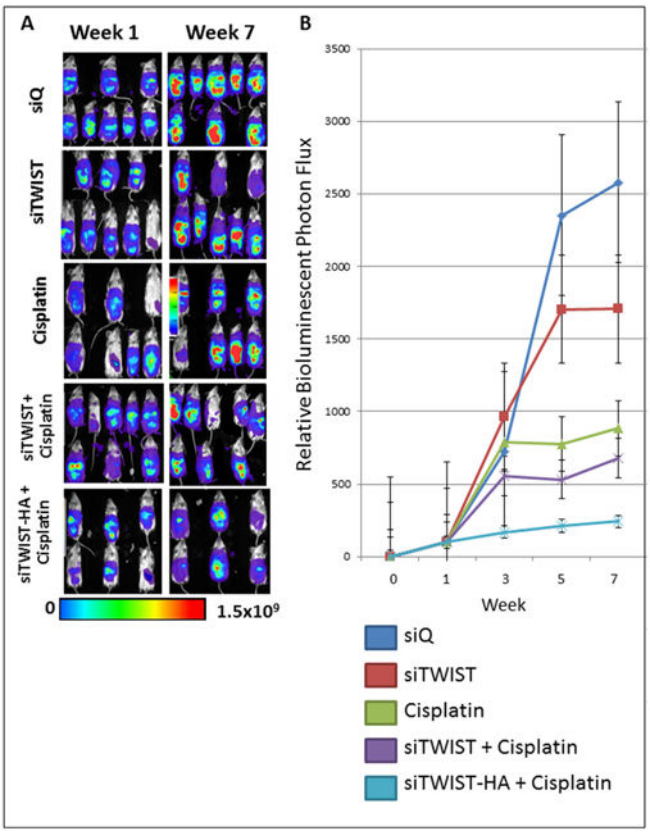

Figure 4.

A. Bioluminescence imaging of Ovcar8-IP tumors. Tumors treated with cisplatin emit noticeably weaker signal than siTWIST or siQ only control mice, while those treated with siTWIST-MSNs plus cisplatin exhibit a further loss of signal. siTWIST-MSN-HAs plus cisplatin exhibit a greatest loss of signal. **B**. Quantification of bioluminescence for all seven weeks of treatment as depicted in A for weeks 1 and 7. Units for luminescence are photons/sec/cm2/steradian.

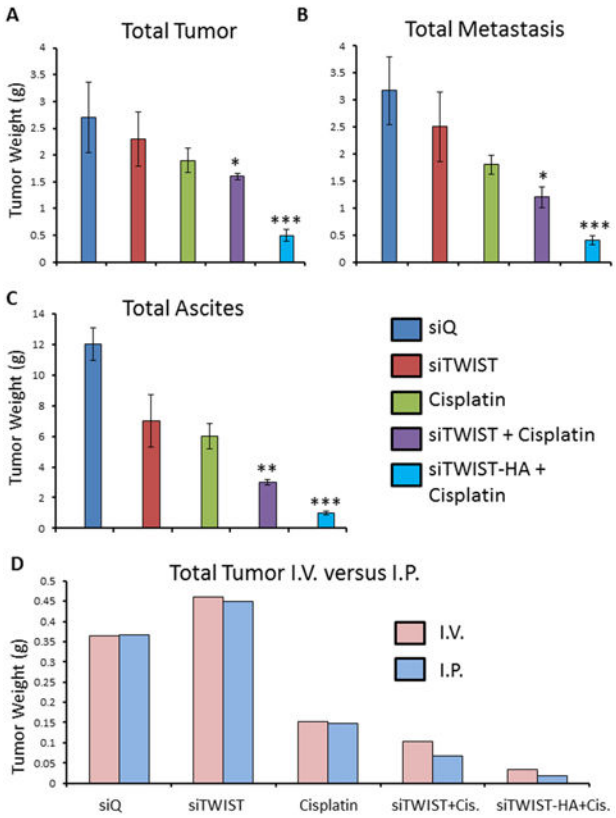

Figure 5.

A. Quantification of total tumor observed in mice. Combination of cisplatin with siTWIST-MSNs reduced tumor burden 20% in comparison to cisplatin alone (P =0.1880); while combination of cisplatin with siTWIST-MSN-HA reduced this 75% (P =0.0012). **B**. Quantification of total metastasis observed. Cisplatin, with or without TWIST knockdown, produced a drop in tumor metastasis compared to controls (siQ and siTWIST). Addition of siTWIST led to a significant decrease (P=0.0084) when compared to cisplatin alone; while combination of cisplatin with siTWIST-MSN-HA reduced this even more (P =0.0011). **C**. Quantification of total ascites collected. Cisplatin, with or without TWIST knockdown, produced a drop in ascites comparing to siQ control. Addition of siTWIST led to a significant decrease (P=0.0072) when compared to cisplatin alone; while combination of cisplatin with siTWIST-MSN-HA reduced this even more (P =0.002). **D**. Quantification of total tumor in grams observed in mice that received therapy via intravenous (IV) versus intraperitoneal (I.P) injection. Results for both delivery vehicles are comparable.

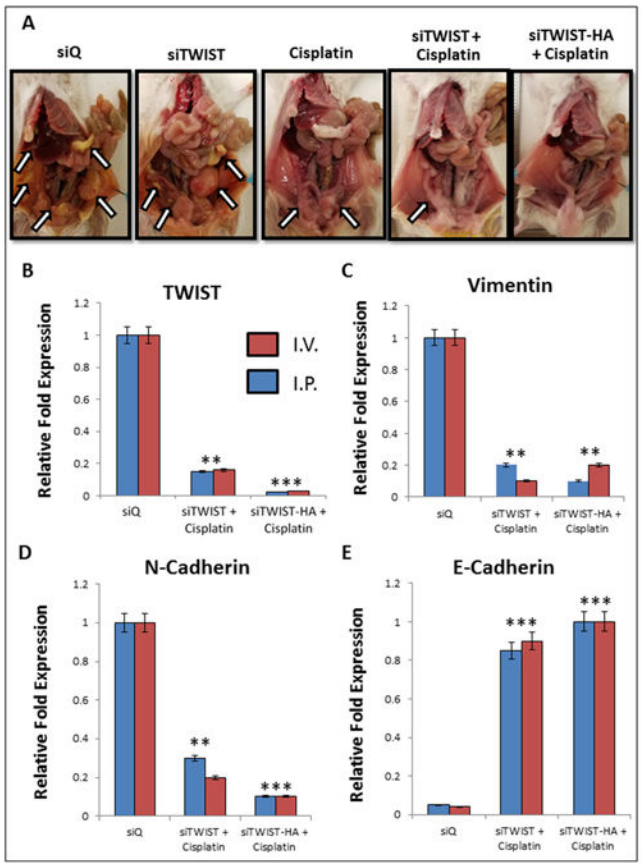

Figure 6.

A. Mice treated with siQ only have greater tumor burden than TWIST knockdown mice. Cisplatin and siTWIST treatment eliminated much of the tumor mass as compared to cisplatin alone, but a combination of cisplatin and siTWIST-MSN-HA knockdown yielded the cleanest peritoneal cavity at the conclusion of the experiment. Arrows indicate tumor foci. One representative image shown per group (siQ, siTWIST and cisplatin n=8; siTWIST and siTWIST-HA n=12). **B.–E.** qPCR results from tumors collected at necropsy. Tumors exhibit loss of TWIST1 (B) and its target genes Vimentin (C) and N-Cadherin (D). In each case, slighty greater knockdown is observed for siTWIST-MSN-HA than siTWIST-MSN alone. E-Cadherin conversely is increased with loss of TWIST (E).

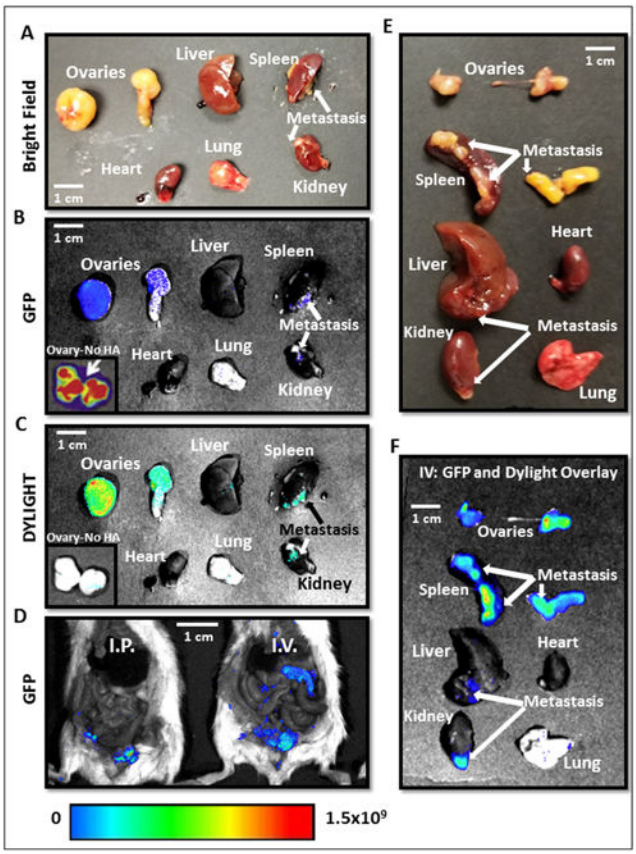

Figure 7.

A.-D. Necropsy images of mice and organs treated with MSN-HA Dylight 680 on consecutive days reveal highly specific tumor localization of siTWIST-MSN-HA complexes as compared to siTWIST-MSN (No HA) alone (C). GFP fluorescence shows all Ovcar8-IP tumor cells within the abdominal cavity (B and D). **E.-F.** Imaging of individual organs reveals that negligible quantities of MSN-HAs are found in the heart, liver, kidney, spleen, or lung. GFP and Diylight fluorescence is nearly all found in disseminated tumors, including lesions on the liver, kidney and spleen surfaces, with most signal emitted from the primary tumor. Units for luminescence are photons/sec/cm^2/steradian.

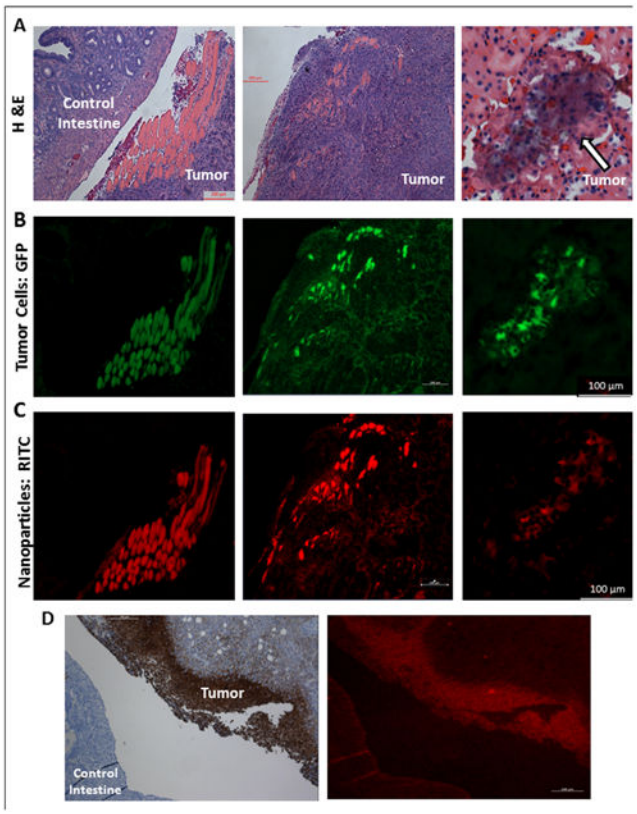

Figure 8.

A. Mouse tumor tissue sections stained with hematoxylin and eosin (H&E) stain after necropsy reveal significant tumor burden. **B.** GFP fluorescence reveals tumor cell location. **C.** RITC fluorescence reveals highly specific nanoparticle tumor targeting; MSN-HA nanoparticles are only localized in tumor cells and not in control intestine. **D.** MSN-HA co-localizes with CD44 on the membrane of tumor.